The Mathematics of Patterns: The modeling and analysis of reaction-diffusion equations

Yayoi Teramoto Kimura

Independent work in partial fulfillment of
the requirements for the certificate in the
Program in Applied and Computational Mathematics
PACM

Advised by:
Dr. Philippe Trinh
Professor Howard Stone

Princeton University
Princeton, New Jersey

May 9, 2014

THE MATHEMATICS OF PATTERNS: THE MODELING AND ANALYSIS OF REACTION-DIFFUSION EQUATIONS

YAYOI TERAMOTO KIMURA

to all those who have taught me
how beautiful math is,
and for all those who
wish to learn

ABSTRACT. Patterns are ubiquitous in nature, and research in the past fifty years have greatly advanced our understanding of the mechanisms through which patterns can originate. The objective of this paper is to review the derivation of models for pattern formation, and the characterization of systems that will develop temporally stable spatial patterns. Special emphasis is made on Turing instabilities, which are the most commonly discussed mechanisms for pattern formation. However, even though the presence of Turing instabilities will be sufficient for pattern formation, there are other types of instabilities that will lead to spatial heterogeneity. In these cases, it is shown that techniques from boundary-layer asymptotic analysis can help study the spatiotemporal dynamics of these non-Turing patterns.

This paper is part of a larger project whose objective was to communicate mathematics to a broader audience. The website that accompanies the paper won first prize in the DSWeb2013 Contest for Teaching Dynamical Systems from the Society for Industrial and Applied Mathematics.

Contents

Acknowledgements

> "What is a teacher? I'll tell you: it isn't someone who teaches something, but someone who inspires the student to give of her best in order to discover what she already knows."
>
> - Paulo Coelho, *The witch of Portobello*

It is not hard to teach, but it is extremely difficult to teach well. Teaching well requires time and a lot of patience, both of which are usually scarce. I, however, was lucky enough to have somebody who was willing to invest both into helping me complete this project. Dr. Philippe Trinh has been a fantastic mentor who has taught me about math, mathematical writing, teaching, and aesthetics. His continued encouragement and support motivated me to get past the roadblocks, and find my way in spite of the (many) changes in direction that this project underwent. This project would have been impossible without him and I will be eternally grateful for everything that he has taught me.

Many thanks to Professor Howard Stone. In addition to being my contact at Princeton when Dr. Trinh was at Oxford, his passion for teaching is an inspiration, and his advice was key in shaping the direction of this project. I would also like to thank my academic advisor Professor Philip Holmes for suggesting this project, and for his many insights in Dynamical Systems. The materials on this website were shaped and inspired by my experience in courses at Princeton that highlighted both the mathematics and the applications of dynamical systems including MAT 323, MAT 350, MOL 215, and MOL 410.

1. Introduction

Pattern formation in nature is a complex process. Just think about the intricate structure of snowflakes, the complex patterning of animal coats, or the geometric designs on seashells. There are even microscopic patterns like the patterns in the connectivity of neurons in the visual cortex in the brain. In spite of their complexity and wide variety, the abundance of patterns in nature suggests that there may be a set of simple principles that govern pattern formation in general. In the past fifty years, researchers have become increasingly interested in understanding the mechanisms of biological pattern formation, and this field has become fertile ground for collaborations between experimental groups and applied mathematicians.

Our understanding of the mathematical principles of pattern formation has been historically linked to research in developmental biology, which deals with one of the most interesting "patterns" in nature: the development of form and structure of developing organisms. The great diversity in body shapes found across the animal kingdom intrigued many researchers. However, the morphological study of organisms shifted away from the evolutionary changes that give rise to the diversity of body traits across species to the developmental processes that allow complex multicellular organisms to arise from single fertilized eggs.

A move towards a more mechanistic and mathematical approach was catalyzed by D'Arcy Thompson's influential book *On Growth and Form* D'Arcy (1992). D'Arcy highlighted the importance of physical laws and first principles that underlie morphogenesis. Even though his approach was theoretical, and he did not provide any experimental data supporting his mechanistic explanations of phenomena in nature, his book shifted the foci of research away from evolution and towards the principles underlying morphogenesis.

One of the great breakthroughs in the field was Alan Turing's paper in 1952, "The chemical basis of morphogenesis" Turing (1952). In this paper, Turing proposed that pattern formation could be understood using a simple system of reaction-diffusion equations representing interacting chemicals. More importantly, the paper suggested that patterns could originate due to the interactions of otherwise stabilizing processes Cooper and Maini (2012). Since then, a lot of experimental and theoretical research has been done to study pattern formation in different contexts, and while some systems will have non-Turing patterns, the intuition and the main components of most models can be traced back to Turing's seminal idea.

1.1. **Structure of the paper and the certificate project.** The goal of this project was to provide a series of multimedia web resources that could supplement a course in dynamical systems. Motivated by several courses at Princeton and Oxford universities, I sought to create a visual guide to the mathematics of pattern formation. The visual nature of the mathematics lent itself to being understood through a series of short movies, animations, audio clips, and illustrations. This paper supplements the videos and website and provides a more complete account of the mathematics of pattern formation.

We begin in §2 by demonstrating how the reaction-diffusion partial differential equation can be derived through a variety of approaches in mathematical modeling. This is continued in §3 where we study a particular type of instability, first proposed by Alan Turing, where small perturbations away from the steady state will drive the system to acquire a temporally stable and spatially heterogeneous profile. In §4 we review the numerical methods that are used to simulate reaction-diffusion equations, and their MATLAB implementation. Finally, we end with a discussion of boundary-layer asymptotic analyses of reaction-diffusion equations in §5, and show that for some systems the patterns observed in numerical simulations will not be Turing patterns.

2. Reaction-Diffusion Equations

In this section, we introduce a class of partial differential equations known as *Reaction-Diffusion Equations*, which are frequently used in modeling and describe the diffusion (spreading out) and reaction of one or several chemical species.

In the simplest one-dimensional case, let $u(x,t)$ be the concentration of some chemical positioned on the real line on x at time t. Then, the reaction-diffusion equation has the form:

$$\frac{\partial u}{\partial t} = D_u \frac{\partial^2 u}{\partial x^2} + f(u), \tag{2.1}$$

where D_u is a coefficient associated with the diffusive properties of u, and $f(u)$ is a function that describes how u grows or decays depending on its current concentration. To understand why these relatively simple equations were first proposed to describe pattern formation and the intuition behind why they present spatial patterns, we present the derivation of the reactive, f, and the diffusive, $D_u u_{xx}$, terms.

2.1. **Reactions.**

A "reaction" often refers to an interaction of some sort between two or more objects, and this is often the case. But in Equation (2.1), what is the lone chemical (whose concentration is u) reacting with? In some sense, a one-dimensional reaction means that the chemical is reacting with zero and is either making more of itself or decaying. A simple example of a decaying reaction corresponds to $f(u) = -u$, and leads to the system,

$$\frac{du}{dt} = -u, \tag{2.2}$$

which has many applications including radioactive decay, and protein degradation. As a result, a more precise interpretation of the reactive term, $f(u)$, is that it describes the change in concentration of u depending on its local value.

It follows that the reactive term $\vec{f}(u)$ for more than one chemical species will describe the local changes in concentrations that are due to the production and decay of each chemical in addition to the interactions between chemicals. Some examples of such reactions are chemical reactions, and population dynamics where two or more species are competing for resources.

2.1.1. *An example of a reaction system.*

Imagine that there is an isolated ecosystem that only contains two species. One species feeds on the vegetation found in the ecosystem, and the second species is a predator that will feed on the first species. In this system, the reactions will be the birth and death rates of each species, and the rate of predation. The most famous predator-prey system is the Lotka-Volterra model Lotka (1925). Letting

U be the number of prey and V be the number of the predator, his model was,

$$\frac{dU}{dt} = a_1 U - a_2 UV, \tag{2.3a}$$

$$\frac{dV}{dt} = a_3 UV - a_4 V, \tag{2.3b}$$

where $a_i, i \in \{1, 2, 3, 4\}$ are growth and decay constants.

We describe the role of each of the terms in (2.3). The $a_1 U$ term indicates that the prey population will grow with rate a_1 (i.e. the rate of reproduction will be proportional to the current population size). The $-a_2 UV$ term corresponds to a decrease in prey population due to predation which has rate a_2. The $a_3 UV$ term indicates that if the predators have food, then they will reproduce. And finally, the $-a_4 V$ term indicates that if the predators do not have food, the predator population will decrease.

It is useful to work with a non-dimensionalised version of the Volterra equations (2.3). Letting,

$$u(\tau) = \frac{a_3 U(t)}{a_4}, \quad v(\tau) = \frac{a_2 V}{a_1}, \quad \tau = a_1 t, \quad a = \frac{a_4}{a_1}, \tag{2.4}$$

we get,

$$\frac{du}{d\tau} = u - uv, \tag{2.5a}$$

$$\frac{dv}{d\tau} = a(uv - v). \tag{2.5b}$$

The evolution of the two (non-dimensionalized) populations over time are shown in Figure 1. The prey population u is graphed on the x-axis and the predator population v is graphed on the y-axis. At a given point (u, v), the arrows in phase space will point in the direction of,

$$\frac{dv}{du} = a\frac{uv - v}{u - uv}, \tag{2.6}$$

We can solve (2.6) exactly to get,

$$au + v - \log(u^a v) = H, \tag{2.7}$$

where H is constant. Thus, u can be solved as a function of v using special functions (in particular, the Lambert W function). It can be shown that for $H > 1 + a$, then we will obtain closed trajectories Murray (2003). Closed trajectories tell us that the populations of u and v will wax and wane over time, but always return to their original state $(u(0), v(0))$.

The set of equations (2.5) has fixed points at $(0, 0)$ and $(1, 1)$. Linearizing about $(0, 0)$, we find that the origin is a saddle. In addition, $(1, 1)$ is neutrally stable, and the

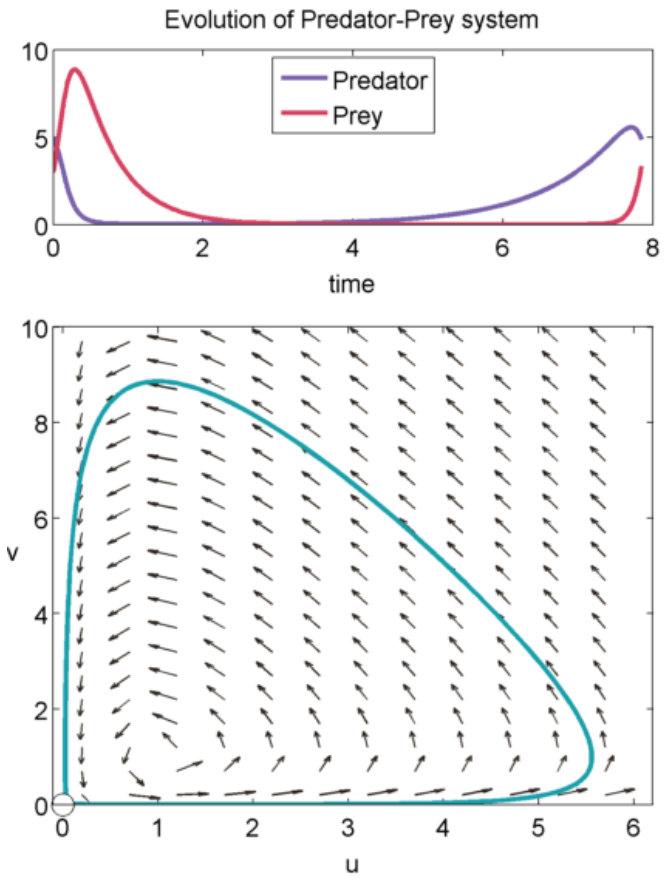

FIGURE 1. **The Lotka Volterra model.** The top panel shows the time evolution of both the predator and prey populations. The bottom panel shows the changes in prey population u in terms of the changes predator population v, and the black arrows point in the direction of dv/du.

solution of the linearised equations about $(1, 1)$ has the form,

$$\begin{pmatrix} \tilde{u}(\tau) \\ \tilde{v}(\tau) \end{pmatrix} = \vec{m}_1 e^{i\sqrt{a}\tau} + \vec{m}_2 e^{-i\sqrt{a}\tau}, \tag{2.8}$$

where $\tilde{u}$ and $\tilde{v}$ are small perturbations away from $(1, 1)$, and $\vec{m_1}$ and $\vec{m_2}$ are the eigenvectors. This solution provides the trajectories illustrated in Figure 1.

2.2. **Diffusion.** The word diffusion comes from the Latin *diffundere* meaning "to pour out" def (2014). Long before it was used to describe a physical phenomenon, "diffusion" was used to describe the dissemination of knowledge, branching out, and a general abstract concept of spreading out. It was not until the 1800s that the term diffusion was used in physics to describe how particles of gases, liquids, and solids intermingle

and move from areas of high concentration to low concentration without chemical combination as a result of each particle's kinetic energy. Adolf Fick described diffusion mathematically, and arrived at this result using a macroscopic approach. In fact, the diffusion equation

$$\frac{\partial c}{\partial t} = D\frac{\partial^2 c}{\partial x^2}, \tag{2.9}$$

is also known as Fick's second law Mehrer and Stolwijk (2009).

There are two well-known approaches to deriving (2.9): we can either derive the transport of species concentration macroscopically, or we can derive the dynamics using stochastic, Brownian motion.

2.2.1. *The macroscopic approach.* Let $c(x,t)$ be the concentration of a chemical, and $q(x,t)$ be its flux. Remember that the flux determines how much chemical will flow through an infinitesimal surface element of area dS with normal $\hat{n}$ in an infinitesimal time interval dt. Thus, the local flux is related to,

$$\text{amount of fluid through } dS = \hat{n} \cdot q(x,t)\ dS\ dt. \tag{2.10}$$

We also assume that the motion of the chemical is governed by *Fick's First Law of Diffusion* which states that the flux is opposite and proportional to the gradient of the concentration by,

$$q = -D\nabla c, \tag{2.11}$$

where $D = D(x,t)$ is the diffusion coefficient and is independent of c and ∇c. (2.11) is an empirical law that describes how substances will flow from areas of high concentration to areas of low concentration.

Through conservation of mass we get that for a fixed closed volume V with a bounding surface ∂V, the change in the total chemical concentration will be the change of concentration of the chemical inside the volume minus the amount of chemicals flowing out of V at any given time. This can be written as,

$$\frac{d}{dt}\int_V c dV = -\int_{\partial V} q \cdot n\ dS. \tag{2.12}$$

Applying equations (2.10) and (2.11) and the divergence theorem we get that,

$$\frac{d}{dt}\int_V c dV = \int_V \nabla \cdot q dv \tag{2.13}$$

$$= \int_V \nabla \cdot (D\nabla c)\, dV. \tag{2.14}$$

Therefore, for any V with surface ∂V we obtain,

$$\int_V \left\{ \frac{\partial c}{\partial dt} - \nabla \cdot (D \nabla c) \right\} dV = 0. \tag{2.15}$$

Since this expression must hold for any arbitrary volume, V, then the integrand must be zero. Thus,

$$\frac{\partial c}{\partial t} = \nabla \cdot (D \nabla c), \tag{2.16}$$

This will simplify to (2.9) assuming that D is a constant.

The microscopic approach. At the macroscopic level, we understand diffusion as causing the substance to spread out according to Fick's Law (and thus moving from areas of high concentration to low concentration).

Brownian motion is named after the British botanist Robert Brown. He described "a peculiar character in the motions of the particles of pollen in water" Brown (1828), and more importantly he stated that this motion is not due to the particles being alive but is instead of a mechanical nature. Albert Einstein, half a century later, proposed a first approximation to Brownian motion from a physical perspective. Einstein's imagined a microscopic particle like one of Brown's pollen particles suspended in liquid. Even though the pollen particle is microscopic, it is much larger than the water molecules, so every time it gets "hit" by the fluid molecules, the particle will move a small amount or each hit. The hits come at random intervals and from all directions Einstein (1956); Nelson (1967). If there are several pollen particles, concentrated in a region of the liquid, random collisions with water molecules will tend to make them spread out, and this is analogous to the 'spreading out' effect of diffusion.

For simplicity, we consider a one-dimensional lattice, where, at point $x = 0, \pm h, \ldots$, we define the *concentration*, $c(x, t)$, as the expected number of particles in position x at time t. The generalization to three-dimensional diffusion is straightforward.

Let us assume first that after some time $t = t + \tau$, each particle moves right or left with equal probability $p/2$, or stays in the same place with probability $1 - p$. The case where $p = 1$ is illustrated in Figure 2. The expected concentration at the next point is:

$$c(x, t + \tau) = \frac{p}{2} c(x - h, t) + \frac{p}{2} c(x + h, t) + (1 - p) c(x, t) \tag{2.17}$$

We now want to generalize from the random walk to the one-dimensional diffusion equations by taking a continuum limit as $h \to 0$ and as $\tau \to 0$. We subtract $c(x, t)$ from both sides of (2.17) to get,

$$c(x, t + \tau) - c(x, t) = \frac{p}{2} [c(x - h, t) + c(x + h, t) - 2c(x, t)]. \tag{2.18}$$

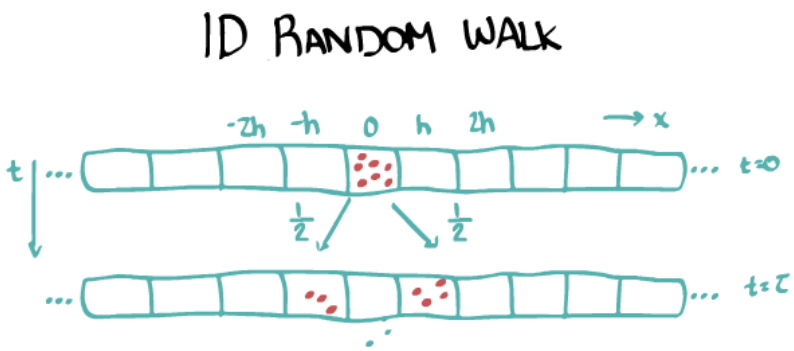

FIGURE 2. **Random Walk.** This figure illustrates a cartoon schematic of random walks along a one-dimensional lattice in the case where particles move right and left with equal probability.

The left hand-side of this equation corresponds to $\tau \partial c/\partial t$ as τ goes to 0, and the right hand-side corresponds to $h^2 \partial^2 c/\partial x^2$ as the discretization of space becomes infinite, *i.e.* h goes to 0. Thus, we are left with,

$$\frac{\partial c(x,t)}{\partial t} = D \frac{\partial^2 c(x,t)}{\partial x^2} \tag{2.19}$$

where D is the *diffusion constant*, and it describes how fast a substance spreads and it takes the form,

$$D = \frac{h^2}{2\tau} \tag{2.20}$$

In Figure 3, we provide an example of the stochastic movement of $N = 10$ particles, that is, at each step in time, $dt = .01$, a random number generator is used to determine whether each of the particles moves left or right.

We can compare with the exact solution of the diffusion equation, which is given by,

$$c(x,t) = \frac{A}{\sqrt{4\pi D t}} \exp\left[-\frac{x^2}{4Dt}\right]. \tag{2.21}$$

The microscopic random walk approximation will be similar to the analytical solution as is shown in Figure 4, where the (2.21) is plotted on top of the distribution of N balls that started at the origin, whose motion was Brownian, and whose final position was binned and plotted as a histogram.

2.3. **A combination of reaction and diffusion.** One of the key questions when studying mathematical models of natural phenomena is where the model came from. Since the goal is to use the mathematical model to understand the principles underlying the phenomenon of interest, it is imperative that the model have a direct relationship

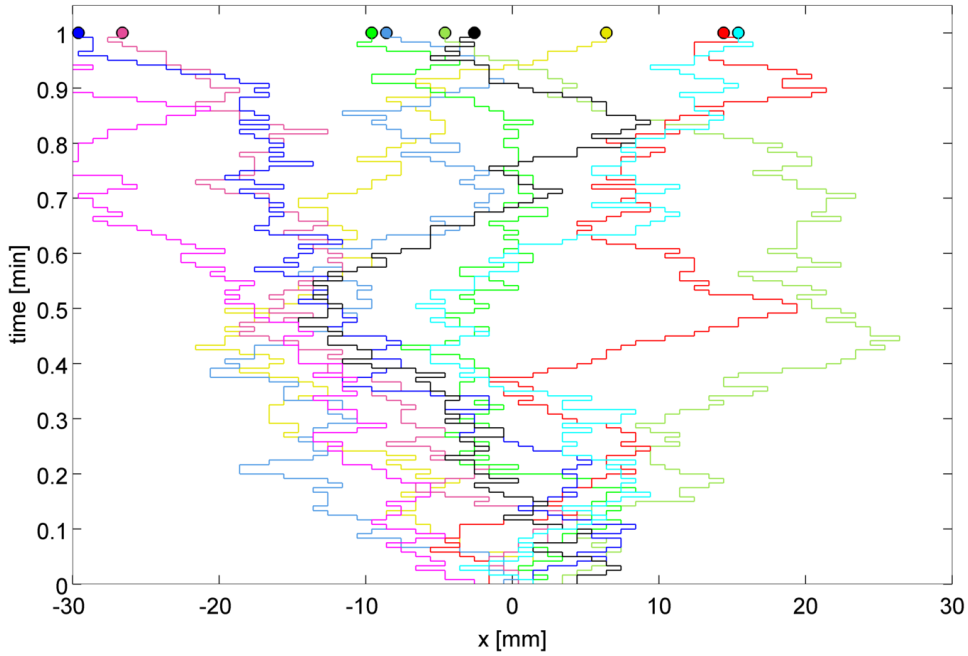

FIGURE 3. **Diffusing particles.** This figure shows the path of ten particles that were started at the origin. At each time step of size $dt = .01$ minutes, the particles will move right or left by $dx = 1$ with equal probability. The simulation is run for one minute and the path of each particle is plotted in the particle's color.

with the system it is modeling. It is thus important to ask why reaction-diffusion models were proposed for pattern formation in the first place.

To understand why reaction-diffusion systems were proposed, we must recall that a lot of the mathematics of pattern formation was developed in the context of development. Alan Turing among other key contributors, were interested in how multicellular organisms could arise from a single cell. One natural question was how embryonic cells differentiated into different cell types that would later form the tissue for different organs. It was posited that chemical gradients throughout the embryo could be one mechanism through which spatial heterogeneity could be achieved. This chemical concentration profile can then influence gene transcription and drive cells to differentiate into different tissue types, which will eventually form the different organs in the body Maini et al. (2012).

The mechanism through which these gradients were set up, however, was not immediately apparent. For a long time, diffusive models had been disregarded because they

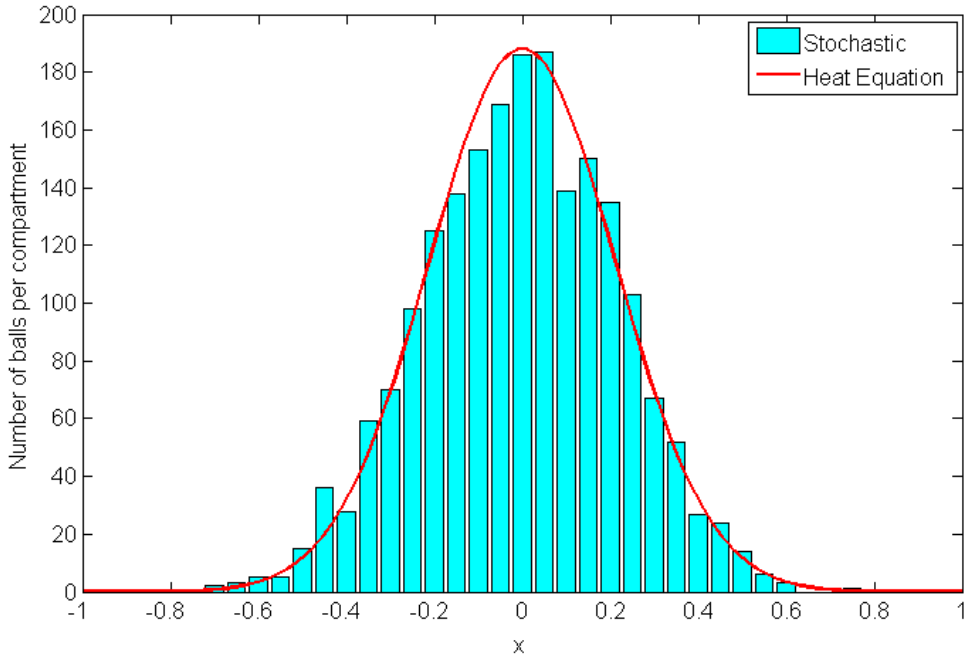

FIGURE 4. **Comparing the heat equation and Brownian motion.** This figure shows the solution to the diffusion equation, or the heat equation, in red. To obtain the teal histogram, 2000 balls with Brownian motion were simulated for 600 time steps. As a result, each bar represents the number of balls whose final position was in that bin.

were assumed to be too slow to establish a stable chemical gradient but this changed in 1970 when Francis Crick modeled diffusion in a one-dimensional embryo and showed that diffusion is sufficiently fast in small domains Crick (1970).
Crick's model was,

$$\frac{\partial C(x,t)}{\partial t} = D\frac{\partial^2 C(x,t)}{\partial x^2}, \tag{2.22}$$

where $C(x,t)$ is the concentration of the chemical at position x and time t. Furthermore, he set the boundary conditions on the 1D embryo of length L to be $C(0,t) = C_0$ and $C(L,t) = 0$.

Crick wanted a stable gradient (in time), so he set the left hand side of (2.22) equal to zero. This system has the form:

$$\frac{\partial^2 C(x,t)}{\partial x^2} = 0, \tag{2.23}$$

and its solution is a straight line.

Finally Crick calculated how much time it would take to reach this stable concentration gradient. From (2.20) we see that the diffusion constant has units [length^2/time]. Thus, the time it takes to set up the gradient is,

$$t = A\frac{(nl)^2}{D}, \tag{2.24}$$

where t is time in seconds, n is the number of cells in the embryo, l is length of each cell in cm, D is the diffusion constant in cm^2s^{-1}, and A is a numerical constant that is fit from the data. Assuming that the time it takes a real embryo to set up the chemical gradient is around three hours, Crick found that diffusion would be fast enough if L was on the order of millimeters, which is the case in fruit flies, which is the animal model used to study this phenomena.

Crick did not have the technology to measure the concentration gradients of any chemicals in the fruit fly embryos, so this was the extent of his analysis. New imaging technologies have been developed that allow scientists to measure the concentration of chemicals in embryos. One very important chemical is called bicoid and it is important in establishing an asymmetry in the anterior-posterior axis (*i.e.* it determines what cells become part of the head and which ones become part of the body) Little et al. (2011). The bicoid gradient does not look linear, and can be better approximated by an exponential curve.

This suggests that the diffusive model alone does not fully explain how chemical gradients are established in the embryo. Thus, models of bicoid usually introduce a reaction term that describes how bicoid is produced and how it degrades as it diffuses across the embryo. This model according to Little et al. (2011) has the following form:

$$\frac{\partial C(x,t)}{\partial t} = D(t)\frac{\partial^2 C(x,t)}{\partial x^2} - \frac{1}{\tau}C(x,t) + \rho(x,t), \tag{2.25}$$

where D is the diffusion constant, τ is the degradation rate, and ρ is a synthesis rate.

Consider a simpler version of (2.25),

$$\frac{\partial C(x,t)}{\partial t} = D\frac{\partial^2 C(x,t)}{\partial x^2} - \frac{1}{\tau}C(x,t), \tag{2.26}$$

which we can solve for a stable gradient analytically,

$$C(x,t) = C_0 e^{-x/\lambda}, \quad \lambda = \sqrt{D\tau} \tag{2.27}$$

This example shows why sometimes reaction and diffusion are needed to make realistic biological models. Diffusion can model spatial phenomena, but often, like in the case of

bicoid, we have local reactions that can only be included in the model with equations like the Reaction-Diffusion PDE in (2.25).

2.4. **Reaction-Diffusion equations and spatial domains.** So far it has been shown that diffusion is very effective in short distances how reaction and diffusion can work together to model experimental data. However, to really understand pattern formation, it is necessary to study the spatial properties of reaction-diffusion equations.

Following Kierstead and Slobodkin (1953), we consider the survival of a phytoplankton population in a body of water. Assume that the phytoplankton can only survive in waters with adequate conditions, and that these regions of water are surrounded by bodies of water where the phytoplankton will die. We ask whether there exists a minimum water mass size where the phytoplankton population will survive?

In the ocean, this water mass would be three-dimensional, but let us take a simpler one-dimensional approach in which we consider a mass of water that has been stretched out into a very thin tube. We impose boundary conditions on the concentration of phytoplankton c such that any phytoplankton at the edges are automatically destroyed, and also that the concentration is constant at $t = 0$. That is, we have the following initial and boundary conditions:

$$c(0,t) = 0 = c(L,t) \tag{2.28a}$$

$$c(x,0) = c_0. \tag{2.28b}$$

Furthermore, assume that the phytoplankton cannot swim so their movement is governed by diffusion. . Therefore, if the phytoplankton population does not grow or decrease, its concentration will be the solution to the diffusion equation which has the form:

$$\frac{\partial c}{\partial t} = D\frac{\partial^2 c}{\partial x^2}. \tag{2.29}$$

However, since phytoplankton are living organisms, we add a reactive term that describes the population growth of the phytoplankton so that Equation (2.29) becomes,

$$\frac{\partial c}{\partial t} = D\frac{\partial^2 c}{\partial x^2} + Kc, \tag{2.30}$$

where K is a growth constant.

Before we solve this using separation of variables, we can simplify our problem by scaling out the diffusion-less exponential growth,

$$c(x,t) = f(x,t)e^{Kt}, \tag{2.31}$$

and substituting Equation (2.31) into Equation (2.30), we find that f must satisfy the standard diffusion (or heat) equation of the previous part,

$$\frac{\partial f}{\partial t} = D\frac{\partial^2 f}{\partial x^2}. \tag{2.32}$$

By the standard techniques of Fourier series, and using the boundary conditions of $c = 0$ at $x = 0, L$, we get that,

$$f = \sum_{n=1}^{\infty} B_n \sin\left(\frac{n\pi x}{L}\right) e^{-n^2\pi^2 D/L^2 t}, \tag{2.33}$$

where B_n are the Fourier sine coefficients given by,

$$B_n = \frac{2}{L}\int_0^L c_0 \sin\left(\frac{n\pi x}{L}\right)\, dx, \tag{2.34}$$

for $n = 1, 2, \ldots$, which are then computed for given initial concentration, c_0.

Substituting (2.32) into (2.31) we get the concentration,

$$c(x,t) = \sum_{n=1}^{\infty} B_n \sin\left(\frac{n\pi x}{L}\right) e^{(K-n^2\pi^2 D/L^2)t}. \tag{2.35}$$

2.4.1. *What will be the steady state of the phytoplankton population?* They key is to note that in (2.35) that because the Fourier coefficients are bounded and decreasing as $n \to \infty$, and the sinusoidals are well behaved, the long term behavior of the system will be controlled by the time term in Equation (2.35), $e^{(K-n^2\pi^2 D/L^2)t}$. In particular, the argument, $K - n^2\pi^2 D/L^2$, will determine whether the population of plankton will grow, stay the same or decay. In particular, if it is exactly zero, the population will be at equilibrium, if the argument is negative, the population will decay over time, and if it is positive, then the population will grow over time.

Moreover, if these conditions hold for the $n = 1$ mode, then the higher modes don't change the steady-state behavior. For $n = 1$, the *bifurcation*, or the point at which the behavior changes from decay to growth, is found at the length, L such that $K - \pi^2\frac{D}{L^2} = 0$.

Therefore, we can get a *critical length* of the form:

$$L_c = \pi\sqrt{\frac{D}{K}}. \tag{2.36}$$

In summary, we have found the critical length of the domain such that for $L = L_c$, the population stays constant, for $L > L_c$, the population increases and for $L < L_c$ the population will decay.

As a final note, observe that the critical length increases proportional to D but inversely proportional to K. This suggests that the steady-state behavior of the plankton population is determined by the relative strength of the diffusive and reactive terms in Equation (2.30). When $L > L_c$ then the reactive term Kc will dominate the long-term behavior, but when $L < L_c$ the diffusive term $D\frac{\partial^2 c}{\partial x^2}$ dominates. When $L = L_c$ the diffusive and reactive forces balance each other equally. (For a more complete discussion on the minimum domains for spatial patterns refer to Murray and Sperb (1983)).

3. Turing instabilities

In 1952, Turing published a paper titled *The chemical basis of morphogenesis* Turing (1952), where he proposed a reaction-diffusion model for pattern formation, in which diffusion was the source of the instability that caused patterns to form. This is counterintuitive, because so far we have studied diffusion as a stabilizing force. However, we will see that the key is that this instability comes from the interaction of the reactive and diffusive terms that govern interacting chemical species that are diffusing within some spatial domain.

3.1. Diffusion-driven instabilities.

Consider the system of equations:

$$\frac{\partial u}{\partial t} = D_u \frac{\partial^2 u}{\partial x^2} + f(u, v), \tag{3.1a}$$

$$\frac{\partial v}{\partial t} = D_v \frac{\partial^2 v}{\partial x^2} + g(u, v). \tag{3.1b}$$

where D_u and D_v are diffusion constants, u and v represent the concentration of two chemical substances and are functions of position and time $u(\vec{x}, t)$, $v(\vec{x}, t)$, and $f(u, v)$ and $g(u, v)$ describe how u and v interact.

We introduce a couple of definitions:

Definition 1: *Patterns* are stable, time-independent, spatially heterogeneous solutions of (3.1).

Definition 2: A *diffusion-driven instability*, or *Turing instability*, occurs when a steady state, stable in the absence of diffusion, becomes unstable when diffusion is present.

Conditions for Turing Instabilities. In this section we derive the conditions needed to obtain (i) stability in the zero-diffusion case so that if the chemicals are not diffusing, or they diffuse at the same rate, they will tend to go to an equilibrium state, and (ii) instability when diffusion is added such that a small perturbation away from equilibrium will lead to a (drastic) change in the spatial structure and patterns will form.

We assume a stationary uniform state (u_0, v_0) exists (i.e. $f(u_0, v_0) = g(u_0, v_0) = 0$).

Let $u(x, t) = u_0 + \tilde{u}$ and $v(x, t) = v_0 + \tilde{v}$, where $\tilde{u}$ and $\tilde{v}$ are small. We can taylor expand about the fixed points to get,

$$f(u, v) = f(u_0, v_0) + \tilde{u}\frac{\partial f(u_0, v_0)}{\partial u} + \tilde{v}\frac{\partial f(u_0, v_0)}{\partial v} + ... \tag{3.2a}$$

$$g(u, v) = g(u_0, v_0) + \tilde{u}\frac{\partial g(u_0, v_0)}{\partial u} + \tilde{v}\frac{\partial g(u_0, v_0)}{\partial v} + ..., \tag{3.2b}$$

so when we linearize (3.1) about (u_0, v_0) we get,

$$\frac{\partial \tilde{u}}{\partial t} = f_u + f_v + D_u \frac{\partial^2 \tilde{u}}{\partial x^2} + ... \tag{3.3a}$$

$$\frac{\partial \tilde{v}}{\partial t} = g_u + g_v + D_v \frac{\partial^2 \tilde{v}}{\partial x^2} + ... \tag{3.3b}$$

For simplicity we can rewrite this in matrix notation as,

$$\frac{\partial}{\partial t}\begin{pmatrix}\tilde{u}\\ \tilde{v}\end{pmatrix} = \left(D\frac{\partial}{\partial x^2} + J_1\right)\begin{pmatrix}\tilde{u}\\ \tilde{v}\end{pmatrix}, \tag{3.4}$$

where,

$$J_1 = \begin{pmatrix} f_u & f_v \\ g_u & g_v \end{pmatrix}, \tag{3.5}$$

and,

$$D = \begin{pmatrix} D_u & 0 \\ 0 & D_v \end{pmatrix}. \tag{3.6}$$

When diffusion is absent, we want our system to be stable. What needs to hold in order for this to be true? The diffusion-less linearized system has the following form:

$$\frac{\partial}{\partial t}\begin{pmatrix}\tilde{u}\\ \tilde{v}\end{pmatrix} = \begin{pmatrix} f_u & f_v \\ g_u & g_v \end{pmatrix}\begin{pmatrix}\delta u\\ \delta v\end{pmatrix}. \tag{3.7}$$

In seeking diffusion-driven instabilities (see Definition 2), we are thus looking for steady-state solutions which are *asymptotically stable*. This requires $Re(\lambda_{1,2}) < 0$, where $\lambda_{1,2}$ are the eigenvalues of J_1.

Recall from linear algebra that in a 2×2 matrix, the trace of the Jacobian $\tau = \lambda_1 + \lambda_2$ and the determinant $\Delta = \lambda_1 \cdot \lambda_2$. Taken together with the fact that $Re(\lambda_{1,2}) < 0$, we get the following two conditions for the stability of (3.7):

$$\tau = f_u + g_v < 0, \tag{3.8a}$$

$$\Delta = f_u g_v - f_v g_u > 0. \tag{3.8b}$$

Now, according to Def. 1, patterns are time-independent and spatially heterogeneous solutions for (3.1). We assume that the solution is separable, so set:

$$\delta\tilde{u}(x,t) = A(t)e^{iqx}, \text{ and} \tag{3.9a}$$

$$\delta\tilde{v}(x,t) = B(t)e^{iqx}, \tag{3.9b}$$

where each q is the wave-number of a Fourier mode.

Then, the diffusion terms become:

$$D_u \frac{\partial^2}{\partial x^2} A(t)e^{iqx} = -q^2 D_u A(t)e^{iqx}, \tag{3.10a}$$

$$D_v \frac{\partial^2}{\partial x^2} B(t)e^{iqx} = -q^2 D_v B(t)e^{iqx}, \tag{3.10b}$$

After we perturb the system by find that the Jacobian for this system is:

$$\frac{\partial}{\partial t}\begin{pmatrix}\delta\tilde{u}\\ \delta\tilde{v}\end{pmatrix} = \begin{pmatrix} f_u - q^2 D_u & f_v \\ g_u & g_v - q^2 D_v \end{pmatrix}\begin{pmatrix}\delta\tilde{u}\\ \delta\tilde{v}\end{pmatrix} \tag{3.11}$$

Equation (3.11) will be unstable when at least one of the two conditions below is true,

$$\tau = f_u + g_v - q^2(D_u + D_v) > 0, \tag{3.12}$$

$$\Delta = (f_u - q^2 D_u)(g_v - q^2 D_v) - f_v g_u < 0. \tag{3.13}$$

Notice that the first condition (3.12) will never be satisfied since $D_u, D_v \in \mathbb{R}^+$ and by (3.8a). Thus, if we want the system to become unstable we need (3.13) to be true.

We look for $q > q_{min}$ where q_{min} is the first mode that can cause an instability, *i.e.* satisfy,

$$H(q^2) = (f_u - q^2 D_u)(g_v - q^2 D_v) - f_v g_u < 0. \tag{3.14}$$

Notice that (3.14) is a quadratic with respect to q^2, so

$$q^2_{min} = \frac{D_u g_v + D_v f_u}{2 D_u D_v}, \tag{3.15}$$

and if we look at where the determinant of the quadratic is positive, we find that:

$$D_u g_v + D_v f_u > 2\sqrt{D_u D_v (f_u g_v - g_u f_v)} \tag{3.16}$$

This may seem a bit too abstract, so in the next section of the notes we will go through an Activator-Inhibitor model known as the Gierer-Meinhardt model.

The previous section derived the conditions that are needed for a Turing instability to exist. Now, let us step through an example in order to see how this works in practice.

3.2. **The Gierer-Meinhardt model.** We consider the Gierer-Meinhardt model, which is a reaction diffusion system that describes an activator-inhibitor interaction which is illustrated in Figure 5.

A simplified form of the original Gierer-Meinhardt model Gierer and Meinhardt (1972) is,

$$\frac{\partial u}{\partial t} = \frac{u^2}{v} - bu + D_u \frac{\partial^2 u}{\partial x^2}, \tag{3.17a}$$

$$\frac{\partial v}{\partial t} = u^2 - v + D_v \frac{\partial^2 v}{\partial x^2}. \tag{3.17b}$$

where we will call u our "activator" and v our "inhibitor", D_u and D_v are diffusion constants, and b is the rate at which the activator u will naturally degrade.

3.2.1. *Stability without Diffusion.* We can picture the diffusionless case of this system as the following picture, where the terms in the equation corresponding to the given connection are written in green:

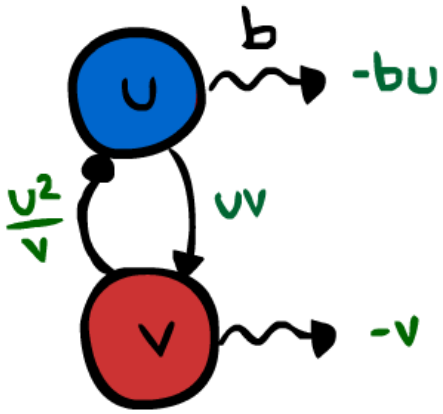

FIGURE 5. **Gierer-Meinhardt model.** This figure shows a schematic of the Gierer-Meinhardt reaction where the activator is shown in blue and the inhibitory is shown in red, and the black arrows show the interaction between the two chemicals and their decay.

Since the diffusion-less model looks like,

$$\frac{\partial u}{\partial t} = \frac{u^2}{v} - bu, \tag{3.18a}$$

$$\frac{\partial h}{\partial t} = u^2 - v, \tag{3.18b}$$

We see that the steady state is given by $u_0 = 1/b$ and $v_0 = u_0^2 = 1/b^2$. Linearizing about the steady state $[u_0, v_0] = [1/b, 1/b^2]$, we find that the Jacobian is,

$$J|_{(1/b,1/b^2)} = \left(\begin{array}{cc} -b + \frac{2u}{v} & -\frac{u^2}{v^2} \\ 2u & -1 \end{array} \right) \Bigg|_{(1/b,1/b^2)} = \left(\begin{array}{cc} b & -b^2 \\ \frac{2}{b} & -1 \end{array} \right). \tag{3.19}$$

Now, it is possible to find the parameter values that will make this a stable equilibria by setting (i) $tr(J) = b - 1 < 0 \Rightarrow b < 1$, and (ii) $det(J) = b > 0 \Rightarrow b > 0$. Therefore $0 < b < 1$.

Instability with diffusion. When we add diffusion to the system we want it to be unstable. In order to study this we add a small perturbation away from the steady state and find the parameter values that will make these small perturbations grow over time.

Let $u(x,t) = u_0 + \tilde{u}$ and $v(x,t) = v_0 + \tilde{v}$, with $\tilde{u}$ and $\tilde{v}$ very small. The linearized system is then used to study $\frac{\partial \tilde{u}}{\partial t}$ and $\frac{\partial \tilde{v}}{\partial t}$.

The linearized system has the form,

$$\frac{\partial \tilde{u}}{\partial t} = b\tilde{u} - b^2\tilde{v} + D_u \frac{\partial^2 \tilde{u}}{\partial x^2}, \tag{3.20a}$$

$$\frac{\partial \tilde{v}}{\partial t} = \frac{2}{b}\tilde{u} - \tilde{v} + D_v \frac{\partial^2 \tilde{v}}{\partial x^2}. \tag{3.20b}$$

The system can be solved by separation of variables as we saw in the previous example, so we look for solutions of the form,

$$\begin{pmatrix} \tilde{u} \\ \tilde{v} \end{pmatrix} = \begin{pmatrix} A(t)e^{iqx} \\ B(t)e^{iqx} \end{pmatrix}, \tag{3.21}$$

where q are the Fourier modes.

The system becomes,

$$\frac{\partial}{\partial t}\begin{pmatrix} \delta\tilde{u} \\ \delta\tilde{v} \end{pmatrix} = \left(\begin{array}{cc} b - q^2 D_u & -b^2 \\ 2/b & -1 - q^2 D_v \end{array} \right) \begin{pmatrix} \delta\tilde{u} \\ \delta\tilde{v} \end{pmatrix} \tag{3.22}$$

We want to find the eigenvalues $\lambda_{1,2}$ of the 2×2 matrix, and we want them to be distinct, and at least one of $Re(\lambda_i) > 0$, $i \in \{1, 2\}$. Thus, we need,

$$det(J) = H(q^2) = (b - D_u q^2)(-1 - D_v q^2) + 2b < 0 \tag{3.23}$$

Notice that the determinant is a quadratic function with respect to q^2, and depending on the value of b it will have zero, one or two real roots. It can be thus seen that we will only get patterns when there quadratic has real silutions.

We will get two real roots for the quadratic when,

$$-bD_v + D_u > 2\sqrt{(D_u D_v)b}. \tag{3.24}$$

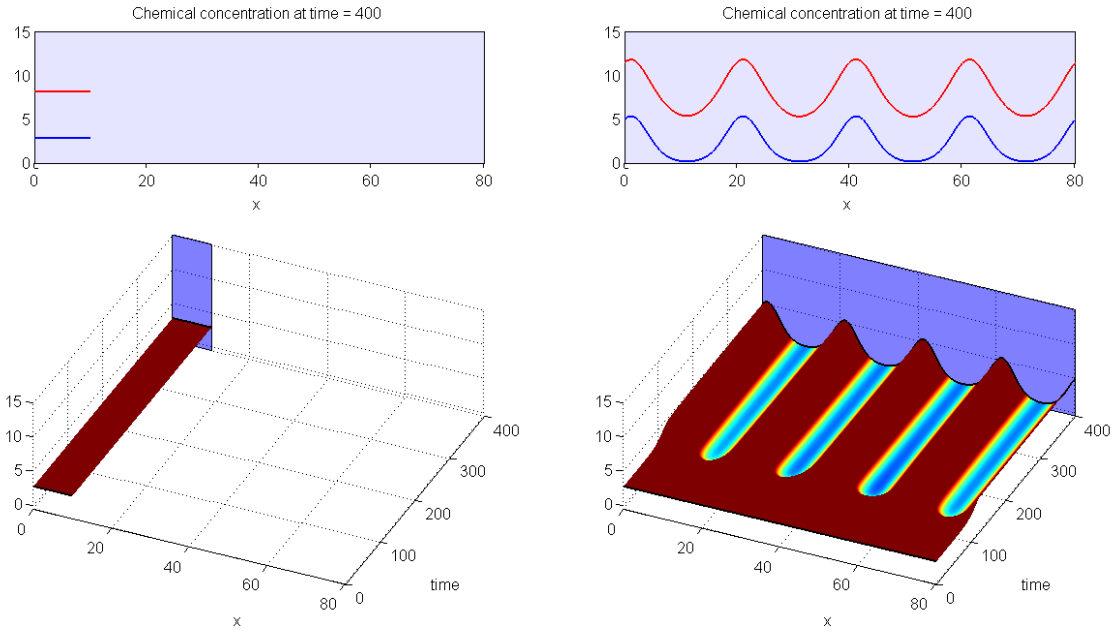

FIGURE 6. **Spatial dependence on patterns.** This figure shows two simulations of the Gierer-Meinhardt system with periodic boundary conditions. The only difference between the two simulations is the spatial domain, and it can be seen that whether or not the system develops spatial patterns depends on the domain.

3.2.2. *Spatial Domain.* If periodic boundary conditions are applied on a domain $x \in [0, L]$, the separable solution will then be of the form

$$\sum_k A_k e^{\lambda(q^2)t} \cos(qx), \tag{3.25}$$

for

$$q = \frac{n\pi}{L}, n \in \{1, 2, ...\}. \tag{3.26}$$

Since we want patterns to form, then the smallest allowed L has to be such that

$$q^2 = \frac{\pi^2}{L^2} > \frac{A + \sqrt{A^2 - B}}{2D_u D_v} = q_+^2, \tag{3.27}$$

where $A = bD_v - D_u$, $B = 4bD_u D_v$, and q_+^2 is the bigger of the two solutions of $H(q^2)$. In other words, our critical length will be $L_c = \frac{\pi}{q_+}$. The dependence on the spatial domain is illustrated by Figure 6.

3.3. **Turing Instabilities and Tiger Stripes.** The systems that we have considered so far are all one-dimensional, but it is not difficult to extend our analysis to two dimensions. In this section we talk of systems that seek to understand the mechanisms through which coat patterns are formed. To do this, we begin by revisiting the spatial dependence of patterns with a 2D Gierer Meinhardt model.

Keeping all parameters the same except for the width of the domain, Figure 7 shows that we obtain stripes on a thin domain with periodic boundary conditions, and spots on the square domain. Recall from the previous section that there was a minimum domain size for the Gierer Meinhardt system to have patterns. In the thin domain, the short edge is not long enough for patterns to form, so we only get patterns in one direction which look like stripes. On the other hand, in the square domain, we get patterns in both directions which results in spots with the parameters used.

This phenomenon was then connected to coat patterns in animal tails by J.D. Murray, who ran simulations of reaction diffusion models on cylindrical domains that tapered off at the ends. (*i.e.* on a trapezoidal surface with periodic boundary conditions on the legs and zero-flux boundary conditions on the bases). He observed that you could get tails that were either entirely striped or that had spots that became stripes at the tip of the tail, similar to the markings observed on the tails of different felines ((Murray, 1988), 3.1 in (Murray, 2003)). This phenomenological model is exciting because it suggests

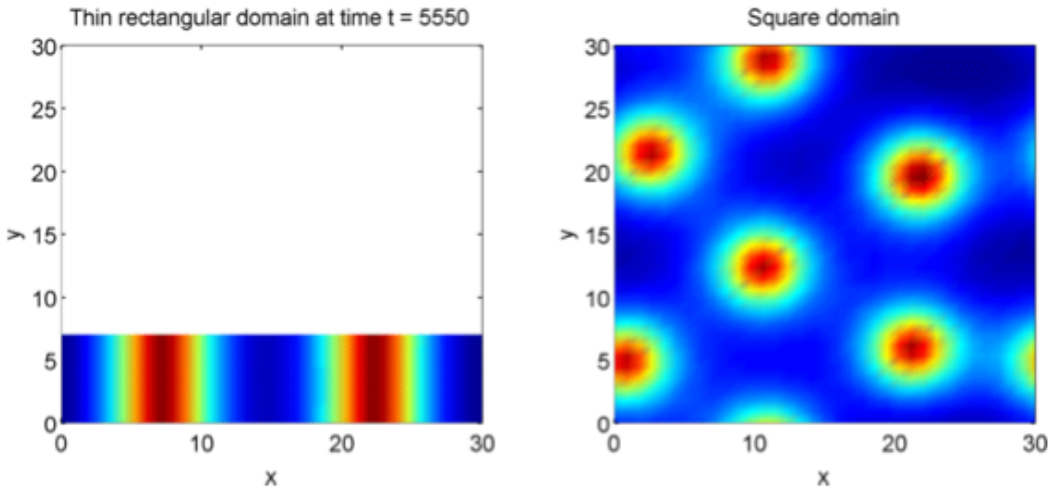

FIGURE 7. **2D Gierer-Meinhardt system.** This figure shows two simulations of a two-dimensional Gierer-Meinhardt system with periodic boundary conditions. The thin domain develops stripes and the square domain form spots.

that if coat patterns are due to the reaction between two (or more) chemical species, the same biological mechanism can result in different patterns (*e.g.* fully striped genet tails and half-spotted half-striped jaguar tails) due to the different sizes of the tails during development (Murray, 1981).

3.4. **Beyond Turing and stripes.** Not all reaction-diffusion systems generate patterns through the same mechanism that was originally proposed by Alan Turing. In addition, small changes in parameters other than just the spatial domain can lead to very different patterns. For example, a very famous system of reaction diffusion equations are the Gray-Scott (GS) equations, which simulate an activator-substrate system; the reaction can be written as:

$$u + 2v \to 3v, \tag{3.28a}$$

$$v \to p. \tag{3.28b}$$

Unlike the Gierer-Meinhardt model which had one chemical acting as an activator, and the other chemical as an inhibitor, the GS system has two chemicals u and v, where v is transformed to an inert product (or substrate) p, and u and v react together to produce more v.

The evolution of the concentration of u and v are described by,

$$\frac{\partial u}{\partial t} = D_u \frac{\partial^2 u}{\partial x^2} - uv^2 + F(1-u), \tag{3.29a}$$

$$\frac{\partial v}{\partial t} = D_v \frac{\partial^2 v}{\partial x^2} + uv^2 - (F+c)v. \tag{3.29b}$$

where D_u, D_v are the diffusion constants as usual, and F, c are constants.

Simulations of the Gray-Scott equations can lead to very different patterns using slightly different parameters as shown below. (*c.f.* Munafo (1998)).

Note that the Gray-Scott equations lead to much more complicated dynamics than the Turing systems, and the patterns that you see are due to the nonlinear interactions between u and v.

4. Numerical solutions of reaction-diffusion equations

Numerical simulations are very useful to understand the behavior of reaction diffusion equations. This section will review some of the key numerical techniques that are used to simulate partial differential equations. The

4.1. **The Heat Equation.**

Recall that the Heat equation (also the diffusion equation) is:

$$\frac{\partial u}{\partial t} - D_u \frac{\partial^2 u}{\partial x^2} = 0, \tag{4.1}$$

where u is temperature, and D_u is a constant that determines how fast heat spreads out. Before we go into the numerics let us step through the solution to the heat equation.

Imagine we have an insulated rod with initial condition $u(x, 0) = u_0$ boundary conditions $u(x, t) = u(L, t) = 0$. We want to solve the PDE in Equation [4.1]. We assume that the solutions are separable, so

$$u(x, t) = T(t)X(x) \tag{4.2}$$

We can substitute this solution into Equation [4.1] to get

$$T'(t)X(x) = D_u T(t)X''(x), \tag{4.3}$$

where the LHS is u_t and the RHS is u_{xx}. Rearranging terms we get,

$$\frac{T'(t)}{D_u T(t)} = \frac{X''(x)}{X(x)}. \tag{4.4}$$

Note that the LHS (left hand side) is a function of time where the RHS (right hand side) is a function of position. In order for this equality to be satisfied for all x and t, we must have that they are both equal to a constant. We let

$$\frac{T'(t)}{D_u T(t)} = \frac{X''(x)}{X(x)} = -\lambda^2, \quad \lambda > 0. \tag{4.5}$$

Solving for each variable we get that ,

$$T(t) = Ae^{-\lambda^2 D_u t} \tag{4.6}$$

$$X(x) = B\cos(\lambda x) + C\sin(\lambda x), \tag{4.7}$$

where A is a positive real constant. We can apply our boundary conditions to find what B and C should be. Since the edges at $x = 0$ is clamped at zero ($u(0, t) = 0$), then $B = 0$. The rod is also clamped at zero at $x = L$, and since $C \neq 0$, then $sin(\lambda L) = 0$ This means that $\lambda_n = \frac{n\pi}{L}$ where $n \in \mathbb{Z}$. Note that (i) $n = 0$ will give a trivial solution,

and (ii) $n \in \mathbb{Z}^-$ just makes all the coefficients negative, so we can just consider the positive values of n without loss of generality.

As a result, we get the following eigenfunctions,

$$u_n(x,t) = A_n e^{-\lambda_n^2 D_u t} sin(\lambda_n x), \quad n = 1, 2, ..., \tag{4.8}$$

with eigenvalues

$$\lambda_n = \frac{n\pi}{L} \tag{4.9}$$

Next, it is necessary to satisfy the initial conditions. Since linear combinations of solutions will still be solutions, then,

$$u(x,t) = \sum_{n=1}^{\infty} A_n e^{-\lambda_n^2 D_u t} sin(\lambda_n x), \tag{4.10}$$

is still a solution. We would like it then, if we could express u_0 as a sum of sine functions as shown in Equation [4.10]. This is true for most u_0 and it is the theory of *Fourier Series*. It can be shown that the *Fourier sine coefficients* are,

$$A_n = \frac{2}{L} \int_0^L u_0(x) sin(\lambda_n x) dx \tag{4.11}$$

However, in general, it is not always easy to obtain solutions to PDE's in closed form, and arguably even Equation (4.9) is not as easy to understand (unless you can visualize an infinite sum!). Instead, we turn to numerical simulations to Partial Differential equations. One of the methods used is known as the finite-difference method. (For a more complete discussion and more MATLAB examples and exercises see (Kharab and Guenther, 2006)).

4.2. **Forward (explicit) method.** One of the difficulties when numerically simulating the heat equation is that (4.1) contains partial derivative in both time and space. We can approximate the partial derivatives of $u(x,t)$ in Eqn. (4.1) as follows:

$$\frac{\partial^2 u}{\partial x^2} \approx \frac{u(x+\Delta x, t) - 2u(x,t) + u(x-\Delta x, t)}{\Delta x^2}, \tag{4.12a}$$

$$\frac{\partial u}{\partial t} \approx \frac{u(x, t+\Delta t) - u(x,t)}{\Delta t}. \tag{4.12b}$$

This finite difference method is also known as the Forward-Time Central-Space method, because at each iteration we approximate the value of u by considering considering the change in space centered around a point in space x using values at $x \pm \Delta x$, and the change in time as in the forward Euler method.

Let n be the index for the time steps, and m be the index for position. We'll also use $k = \Delta t$ and $h = \Delta x$, and write $u(m, n) = u_m^n$

Then, he heat equation can be solved numerically by using the following,

$$\frac{1}{k}\left(u_m^{n+1} - u_m^n\right) = \frac{1}{h^2}\left(u_{m-1}^n - 2u_m^n + u_{m+1}^n\right) \tag{4.13a}$$

$$u_m^{n+1} = u_m^n + \frac{k}{h^2}\left(u_{m-1}^n - 2u_m^n + u_{m+1}^n\right) \tag{4.13b}$$

$$u_m^{n+1} = \frac{k}{h^2}u_{m-1}^n + \left(1 - \frac{2k}{h^2}\right)u_m^n + \frac{k}{h^2}u_{m+1}^n. \tag{4.13c}$$

Now, let us consider the behavior at the edges of the rod. Let us discretize our rod at M points, $u_1^n, u_2^n, ..., u_{M-1}^n, u_M^n$. Notice that (4.13c) will work at every position along a one-dimensional rod except for the two edges (at u_1 and u_M), because there are no values for u_0 and u_{M+1} to approximate the centered finite difference. This requires us to add boundary conditions, and in this section we consider periodic boundary conditions. This means that $u_1^n = u_M^n$, so:

$$u_0^n = u_{M-1}^n, \tag{4.14a}$$

$$u_{M+1}^n = u_2^n \tag{4.14b}$$

It is convenient to rewrite (4.13c) as a matrix operation,

$$\vec{u}^{n+1} = B\vec{u}^n, \tag{4.15}$$

where $\vec{u}^n$ are the values of u at time n for all values $x_1, ..., x_M$, and

$$B = \begin{pmatrix} a & b & 0 & \dots & b & 0 \\ b & a & b & \dots & 0 & 0 \\ 0 & b & a & \ddots & & 0 \\ 0 & & \ddots & \ddots & \ddots & \vdots \\ \vdots & & & b & a & b \\ 0 & b & \dots & 0 & b & a \end{pmatrix}, \tag{4.16}$$

where $a = 1 - \frac{2k}{2}$, and $b = \frac{k}{h^2}$, and where B is a tridiagonal matrix except at $B_{1,M-1} = B_{M,2} = b$ that satisfies the boundary conditions.

4.3. **Backward (implicit) method.** The forward method does not guarantee stability. As a result, it is often convenient to use Implicit methods, which are stable, and which will allow you to take larger time steps, even though the 'accuracy' of the simulation will still depend on the size of the time step.

The idea is the same, but the algorithm is as follows,

$$\frac{1}{k}\left(u_m^{n+1} - u_m^n\right) = \frac{1}{h^2}\left(u_{m-1}^{n+1} - 2u_m^{n+1} + u_{m+1}^{n+1}\right) \tag{4.17a}$$

$$u_m^n = -\frac{k}{h^2}u_{m-1}^{n+1} + \left(1 + \frac{2k}{h^2}\right)u_m^{n+1} - \frac{k}{h^2}u_{m+1}^{n+1}. \tag{4.17b}$$

We can write (4.17b) as a product of matrices to get

$$\vec{u}^n = B'\vec{u}^{n+1}, \tag{4.18}$$

where B' has the same form as B in (4.13c) but with $a = 1 + \frac{2k}{h^2}$ and $b = -\frac{k}{h^2}$

Then, at each step we need to solve Equation (4.18) for $\vec{u}^n$ so:

$$\vec{u}^{n+1} = B'^{-1}\vec{u}^n \tag{4.19}$$

4.4. **Adding in the reaction term.** Let us now see how to update our value of u, when we are looking at a Reaction-Diffusion system like,

$$\frac{\partial u}{\partial t} = D\frac{\partial^2 u}{\partial x^2} + f(u). \tag{4.20}$$

Recall that if we just had,

$$\frac{\partial u}{\partial t} = f(u), \tag{4.21}$$

then we simulate it using the forward Euler method so,

$$\vec{u}^{n+1} = f(\vec{u}^n)\,k. \tag{4.22}$$

where $k = \Delta t$.

Therefore, for the explicit method, we combine (4.15) and (4.22) to obtain that the update at each time step is,

$$\vec{u}^{n+1} = B\,\vec{u}^n + f(\vec{u}^n)\,k \tag{4.23}$$

If we use the implicit method for the diffusion, and the explicit method, then we need to solve

$$B'\,\vec{u}^{n+1} = \vec{u}^n + f(\vec{u}^n)\,k, \tag{4.24}$$

for $\vec{u}^{n+1}$. Thus, at each step we need to compute,

$$\vec{u}^{n+1} = B'^{-1}\,(\vec{u}^n + f(\vec{u}^n)\,k). \tag{4.25}$$

4.5. **MATLAB code examples.** The following code is an example of how to use these methods in MATLAB .

```
%%%%%%%%%%%%%%%%%%%%%%%
%%% Screencast code %%%
%%%%%%%%%%%%%%%%%%%%%%%


%%% Forward Finite difference method %%%

% At each time step compute: u(n+1) = B u(n)
% How do we create B in MATLAB?

% Parameters
D = 2;                % Diffusion constant
dx = 0.2; dt = 0.1;   % space and time step
Nx = 6;               % Number of grid points

% Making the Matrix
a = (1-2*D*dt/dx^2); % Diagonal values
b = D*dt/dx^2;       % Off-diagonal values
main = a*sparse(ones(Nx,1));
off  = b*sparse(ones(Nx-1,1));
B = diag(main) + diag(off,1) + diag(off,-1); % Make B
% Apply periodic boundary conditions
B(1, end-1) = b;
B(end, 2) = b;


% Useful MATLAB functions we used
    % diag
    % imagesc
    % sparse
```

The next code will create the plots that were used to make the figures in §3.

```
% The Mathematics of Patterns 2013
% Turing Instabilities II: Gierer Meinhardt system in 1D

% This MATLAB code will show you how to numerically simulate
% the 1D Gierer-Meinhardt system, and create a simplified
% version of the animations in the Turing Instabilities section.
clear all
close all

%%%%%%%%%%%%%%%%%%%%%
%%%    Set-up     %%%
%%%%%%%%%%%%%%%%%%%%%

% Parameter values
bc  = 0.35;
Du = 1;   Dv = 30;  % Diffusion constants

% Grid and initial data:
% w = 10;  %no pattern
w = 80;  % pattern

Nx = 500; % How many points we want to discretize our domain with
x = linspace(0,w, Nx);
dx = x(2) - x(1);

dt = 1; % size of our time step
t = 0:dt:400;
Nt = length(t); % Number of time points

% Set up for the surface
[X, T] = meshgrid(x, t);
U = 0*X;
V = 0*X;

% Easier to deal with column vectors
x = x(:);
t = t(:);

```

```
%Initial conditions: small perturbation away from steady state
u = 1/bc*ones(length(x),1) + 0.01*rand(Nx, 1);
v = 1/bc^2*ones(length(x),1);

% Save initial conditions
U(1,:) = u;
V(1,:) = v;


%%%%%%%%%%%%%%%%%%%%%%%%%
%%% Making the matrix %%%
%%%%%%%%%%%%%%%%%%%%%%%%%

% To begin, let us recall how to set up the matrices used in the ...
    explicit
% and implicit finite difference methods.


%%% Forward (explicit) method %%%
% We want a tridiagonal matrix (see notes for details)
a = (1-2*Du*dt/dx^2);  % values along the diagonal
b = Du*dt/dx^2;        % values in the off-diagonal
main = a*sparse(ones(Nx,1));
off  = b*sparse(ones(Nx-1,1));
Bu = diag(main) + diag(off,1) + diag(off,-1); %Still a sparse matrix
% Satisfying boundary conditions
Bu(1, end-1) = b;
Bu(end, 2) = b;

% To have a more numerically stable code, we use the implicit method.

%%% Backward (implicit) method %%%
% For u
    a = (1+2*Du*dt/dx^2);  % values along the diagonal
    b = Du*dt/dx^2;        % values in the off-diagonal
    main = a*sparse(ones(Nx,1));
    off  = -b*sparse(ones(Nx-1,1));
    Bu = diag(main) + diag(off,1) + diag(off,-1); %Still a sparse ...
        matrix
    % Satisfying boundary conditions
    Bu(1, end-1) = -b;
```

```
78      Bu(end, 2) = -b;
79
80  % Same thing for v
81      a = (1+2*Dv*dt/dx^2); b = Dv*dt/dx^2;
82      main = a*sparse(ones(Nx,1));
83      off  = -b*sparse(ones(Nx-1,1));
84      Bv = diag(main) + diag(off,1) + diag(off,-1);
85      Bv(1, end-1) = -b;
86      Bv(end, 2) = -b;
87
88  %%%%%%%%%%%%%%%%%%%%%%%%
89  %%%      Plotting      %%%
90  %%%%%%%%%%%%%%%%%%%%%%%%
91
92  figure(1); %create new figure
93  plot(x,u,'g.-', 'linewidth',1);
94  hold on;
95  plot(x,v,'r.-', 'linewidth',1);
96  hold off;
97
98  axis([-1 80 -.01 15.01])  % Fix axis limits
99
100 for j = 1:Nt
101     % f and g are the reaction terms in the G-M system
102     f = u.^2./v-bc*u;
103     g = u.^2 - v;
104
105     % At each step we need to solve the system
106     u = Bu\(u + dt*f);   % backward Euler
107     v = Bv\(v + dt*g);
108
109     % Plot
110     plot(x,u,'g.-', 'linewidth',1);
111     hold on;
112     plot(x,v,'r.-', 'linewidth',1);
113     hold off;
114     axis([-1 80 -.01 15.01])
115     title(['t = ', num2str(j*dt)],'fontsize',24)
116     drawnow;
117
118     % Save for surface
```

```
    U(j,:) = u;
    V(j,:) = v;
end


%%%% Plotting the surface %%%%
figure(2);
s = surf(x, t, U)
set(s, 'EdgeColor', 'none', 'FaceColor', 'interp');
% Sets up the colors
xlabel('x')
ylabel('t')
zlabel('u')

%%%% contour plot %%%
figure(3);
p = pcolor(x, t, U);
set(p, 'EdgeColor', 'none', 'FaceColor', 'interp');
```

5. Asymptotic analysis of localized spots

5.1. **Does the story end with Turing Instabilites?** The theory for patterns that we have been developing until now works for systems that, when linearized about the steady state, turn out to be unstable due to the reactive and diffusive interactions of two 'chemical' species. However, there are systems that can exhibit pattern formation but that do not satisfy all the conditions for a Turing instability. What is happening in these systems? Where does our method fail?

Recall from past sections that systems with Turing instabilities only require a small perturbation away from the steady state to form patterns. But what if patterns will only form when there is a large perturbation away from the equilibrium state? Our local analysis will no longer be sufficient to reveal the pattern forming behavior of the system. So what can we do in these cases?

The reason why most texts on pattern formation stop at Turing instabilities is that the analysis of these more complicated systems require more advanced mathematics. One set of mathematical tools that we can use are asymptotic approximations of the solutions to the system.

5.2. **Motivating example.** To motivate the use of this method, let us look at the following example.

$$u_t = \epsilon^2 u_{xx} - u + \frac{u^3}{v^2} \tag{5.1a}$$

$$\tau v_t = D v_{xx} - v + \frac{1}{\epsilon} u^3 \tag{5.1b}$$

$$u_x = v_x = 0, \quad x = \pm 1. \tag{5.1c}$$

Here, we have that the activator u diffuses much more slowly than the inhibitor v, and it is in exactly the same form as the reaction diffusion equations we studied before.

To begin, let's see whether this system will have Turing instabilities.

Linearizing about its fixed point at (0,0) we get that the Jacobian of the diffusion-less system is,

$$\begin{bmatrix} -1 & 0 \\ 0 & -1 \end{bmatrix}. \tag{5.2}$$

The trace is negative and the determinant is positive so it is stable with no diffusion.

However, the third condition for a Turing Instability is that it must satisfy (3.16). However, when we substitute in the values for our system we get that $-(\epsilon^2 + D) > 0$, but since $\epsilon^2 > 0$, and $D > 0$ this is a contradiction. According to this, we would expect no patterns to form, but the system does present patterns in the form of localized spots.

5.3. **Boundary Layer Analysis.** To begin, it is convenient to understand what we are doing when we linearize. By doing a Taylor expansion and ignoring higher order terms, our underlying assumption is that most of the behavior of our system will be captured by the leading order.

So, if we expand,

$$u = u_0 + \epsilon u_1 + ..., \quad v = v_0 + \epsilon v + ... \tag{5.3}$$

we can substitute into our system, and get that at leading order,

$$u_{0t} = -u_0 + u_0^3/v_0^2 \tag{5.4a}$$

$$u_0^3 = 0 \tag{5.4b}$$

Naively we would say that $u_0 \to 0$ and $v_0 \to$ constant. However, this is only what happens most of the time. At certain values of x, our naive asymptotic analysis will break down and this is known as a *boundary layer*.

The intuitive way to think about what we are going to do next is as follows. For most values, our naive analysis will be okay, but around certain values, that solution will not be appropriate. Thus, we want to use our simple solution above as much as possible, and smoothly 'stitch' the solution around the special values of x that better describe the behavior of the system in the neighborhood of x. Thus, if we posit that there is a boundary layer around a point $x = x_0$, we divide our analysis into the inner and outer parts.

5.3.1. *Inner analysis.* Near $x = x_0$, our analysis breaks down because the change in concentration of the chemical species begins to change very fast. In other words, we can no longer ignore higher order terms. As a result, we need to re-scale the equation near $x = x_0$, and we propose a new variable,

$$y = \frac{x - x_0}{\epsilon}, \tag{5.5}$$

which is O(1) when x is located $O(\epsilon)$ away from x_0. For simplicity assume that x_0 is fixed, even though this is not quite the case.

We propose an inner solution $u(x,t) = U(y)$, and $v(x,t) = V(y)$, where we assume that the solutions are quasi-steady, so they do not depend on time. The derivatives for both become:

$$\frac{d}{dx} = \frac{dy}{dx}\frac{d}{dy} = \frac{1}{\epsilon}\frac{d}{dy}. \tag{5.6}$$

This reflects the fact that as we approach x_0, the derivatives in x became very large, so that terms that we originally dismissed as being small because they were scaled by ϵ are now large, so we have to take them into account.

We do an asymptotic expansion around the variables in terms of y,

$$U = U_0 + \epsilon U_1 + ..., \quad V = V_0 + \epsilon V_1 + ... \tag{5.7}$$

The leading order is now,

$$0 = U_{0yy} - U_0 + U_0^3/V_0^2 \tag{5.8a}$$

$$0 = DV_{0yy} \tag{5.8b}$$

By integrating the second equation twice, we get that $V_0 = Ay + B$ for constants A and B. However, our outer solution $v_0(x)$ with $x \to x_0$ approaches a well-defined number so we need $V_0(y) \to v_0(x_0)$ as $y \to \infty$. Therefore,

$$V_0(y) = B = v_0(x_0), \tag{5.9}$$

where we will determine the value of $v_0(x_0)$ in a later section.

First, to determine $U(y)$, we recall from (5.8a),

$$0 = U_{0yy} - U_0 + U_0^3/V_0^2.$$

Let $U = V_0 w$, then substituting into the (5.8a), U will become,

$$w'' - w + w^3 = 0, \tag{5.10}$$

The solution can be verified to be

$$w(y) = \sqrt{2}\text{sech}(y), \tag{5.11}$$

since by the boundary conditions we need $w(y) \to 0$ as $y \to \infty$ and by assuming the spike is positive and symmetric, this further constrains the differential equation to satisfy $w'(0) = 0, w > 0$.

Therefore, we have that the inner solutions are,

$$V_{inner}(y) \sim \text{constant} = v_0(x_0) \tag{5.12a}$$

$$U_{inner}(y) \sim \sqrt{2}\text{sech}(y) = \sqrt{2}\text{sech}\left(\frac{x-x_0}{\epsilon}\right) \tag{5.12b}$$

5.3.2. *Finding V_0.* In order to find V_0, we propose a uniformly valid solution, meaning that this solution is valid both away from $x = x_0$ and near the boundary layer. This requires us to find the effect of the spike solution on the outer solution.

Recall that in (5.1) the term v^3/ϵ was used to argue that $v \sim 0$. However, this is not true in the boundary layer. In particular,

$$\frac{1}{\epsilon}V_0^3 w\left(\frac{x-x_0}{\epsilon}\right)^3 \to \begin{cases} 0 & \epsilon \to 0, x \neq x_0 \\ \infty & \epsilon \to 0, x = x_0. \end{cases} \tag{5.13}$$

It can be shown that the spike inner solution with w is a regularization of a delta function. Thus, we write,

$$\frac{1}{\epsilon}V_0^3 w^3 \sim \frac{1}{\epsilon}\left(\int_{-1}^{1} V_0^3 w^3\, dx\right)\delta(x-x_0) = V_0^3\left(\int_{-\infty}^{\infty} w^3 dy\right)\delta(x-x_0). \tag{5.14}$$

The outer solution $v \sim V_0$ satisfies

$$DV_{0xx} - V_0 = V_0^3\left(\int_{-\infty}^{\infty} w^3\, dx\right)\delta(x-x_0) \tag{5.15a}$$

$$V_{0x} = 0 \quad \text{at } x = \pm 1. \tag{5.15b}$$

Therefore, we need to solve

$$Dv'' - v = C \cdot \delta(x-x_0), \tag{5.16}$$

where $C = V_0^3\left(\int_{-\infty}^{\infty} w^3 dy\right) > 0$ Looking at the left hand side we see that we need,

$$Dv_L'' - v_L = 0 \tag{5.17a}$$

$$Dv_R'' - v_R = 0 \tag{5.17b}$$

Since $v_L'(-1) = v_R'(1) = 0$, we see that the solution will have the form,

$$v_L = c_1\text{cosh}\left(\frac{x+1}{\sqrt{D}}\right), \tag{5.18a}$$

$$v_R = c_2\text{cosh}\left(\frac{x-1}{\sqrt{D}}\right). \tag{5.18b}$$

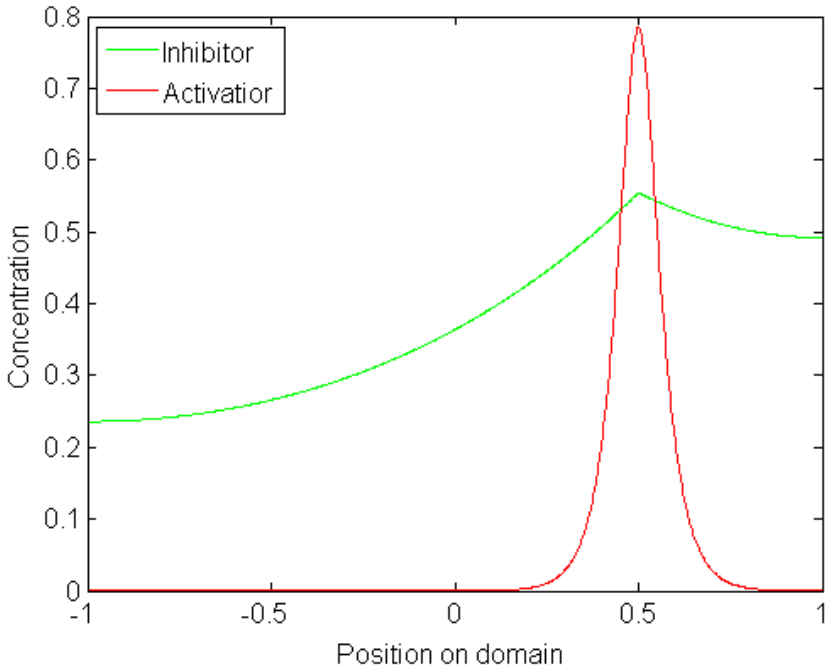

FIGURE 8. **Using boundary-layer asymptotic analysis.** The figure shows the spatial profile of the chemical concentrations of the inhibitor and the activator for $\epsilon = 0.05$.

In addition we have the following jump conditions. As $x \to x_0$, $Dv'' \sim -C\delta(x - x_0)$, so Dv'
$sim - cH(x - x_0)$ where $H(x)$ is the heaviside equation. It follows that the jump condition will be $[v']_-^+ = -C/D$.

Note that since,

$$Dv \sim -C \int^x H(s - x_0)ds, \tag{5.19}$$

is continuous, then v will be continuous at $x = x_0$.

Therefore, we solve

$$V_L(x_0) = V_R(x_0) \tag{5.20a}$$

$$V_R'(x_0) - V_L'(x_0) = -C/D = \frac{V_0^3 \left(\int_{-\infty}^{\infty} w^3 dy\right)}{D}. \tag{5.20b}$$

The solution of this equation can be verified to be,

$$v_L(x) = A\ C\ \cosh\left(\frac{x+1}{\sqrt{D}}\right) \tag{5.21a}$$

$$v_R(x) = B\ C\ \cosh\left(\frac{x-1}{\sqrt{D}}\right) \tag{5.21b}$$

$$A = \frac{\cosh\left(\frac{x_0-1}{\sqrt{D}}\right)\operatorname{csch}\left(\frac{2}{\sqrt{D}}\right)}{\sqrt{D}} \tag{5.21c}$$

$$B = \frac{\cosh\left(\frac{x_0+1}{\sqrt{D}}\right)\operatorname{csch}\left(\frac{2}{\sqrt{D}}\right)}{\sqrt{D}}. \tag{5.21d}$$

The solution is plotted in Figure 8.

5.4. **Studying the dynamics of spikes.** So far the analysis has focused on the case where the boundary layer is time-independent. However, if we suppose instead that $x_0 = x_0(\epsilon^\alpha t)$ where $\alpha \in \mathbb{Z}^+$, such that

$$y = \frac{x - x_0(\epsilon^\alpha t)}{\epsilon} \tag{5.22}$$

Then,

$$\frac{\partial}{\partial x} \to \frac{1}{\epsilon}\frac{\partial}{\partial y} \tag{5.23a}$$

$$\left.\frac{\partial}{\partial t}\right|_x = \left.\frac{\partial}{\partial t}\right|_y + \frac{\partial y}{\partial t}\frac{\partial}{\partial y} \tag{5.23b}$$

$$\frac{\partial y}{\partial t} = -\frac{1}{\epsilon}\cdot\frac{\partial}{\partial t}(x_0(t^\alpha t)) \tag{5.23c}$$

$$= -\frac{1}{\epsilon}\dot{x}_0(t^{\alpha+1})\frac{\partial \tau}{\partial t} \tag{5.23d}$$

$$= -\frac{\epsilon^\alpha}{\epsilon}\dot{x}_0(t^{\alpha+1}) \tag{5.23e}$$

Recall (5.1a). Changing variables, we get that in the inner region,

$$U_t - \epsilon^{\alpha-1}\dot{x}_0(t^{\alpha+1})\frac{\partial u}{\partial y} = U_{yy} - U + U^3/V^2, \tag{5.24}$$

Note that we want to involve the time term so we want $\alpha = 2$. This leads to the prediction that the spike will move proportional to ϵ^2. To verify this empirically, we can run simulations and plot the change in the location of the spike center x_0, which is shown in Figure 9. We find that the movement of the peak is on the order of $\epsilon^2 t = \mathcal{O}(1)$.

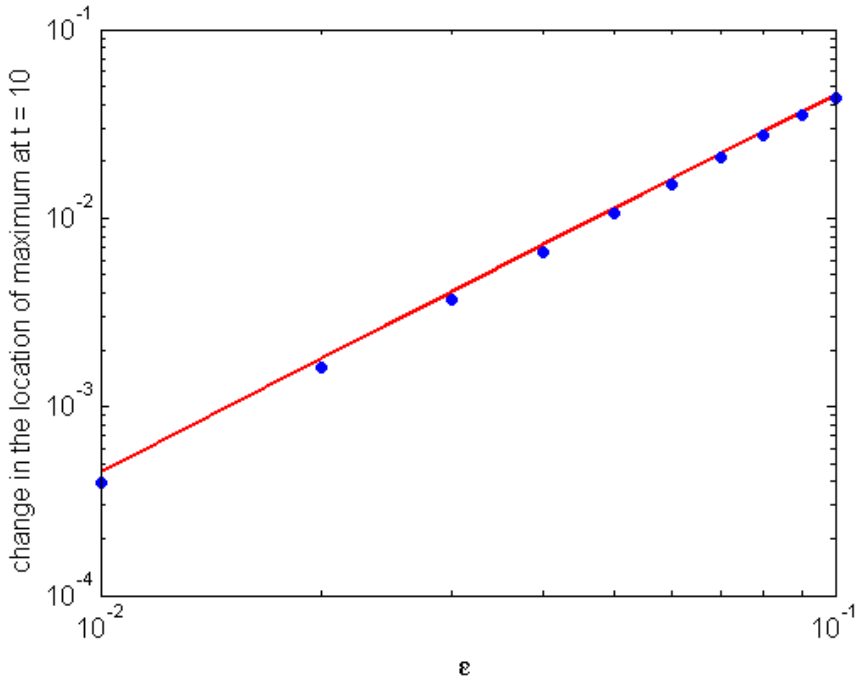

FIGURE 9. **Slow spike dynamics.** The figure shows the amount of drift in the peak of the localized spike as a function of ϵ, and a line of slope 2 is fitted to the data. This suggest that the motion of the localized spike is $\mathcal{O}(\epsilon^2)$.

This means that time must increase by $1/\epsilon^2$ to see the peak move, and since $\epsilon << 1$, then the spike will in fact be quasi-stable.

6. Discussion

The canonical reaction diffusion model of pattern formation was developed because many patterns will form in systems that contain two competing elements which are often assumed to be chemicals. In order to gain a better understanding of the patterns that are formed during development, many models have been extended to study patterns in growing domains Maini et al. (2012). Furthermore, there are many variations of reaction diffusion equations have been developed to model different coat patterns in nature including those in (i) fish (*c.f.* Kondo (2009), Nakamasu et al. (2009)), (ii) snakes (*c.f.* Murray and Myerscough (1991)), and (iii) leopards (*c.f.* Murray (1988) and chapter Murray (2003)).

The purpose of mathematical models are to reach a deeper understanding of the complex phenomena seen in nature, so all models, by definition, are false. However, one of the biggest criticisms that the mathematical models for pattern formation have received is that they are "too false", because they are all phenomenological and have little experimental evidence that makes the reaction-diffusion model biologically plausible. The reaction-diffusion models we have studied in these notes have a lot of attractive points (*e.g.* they generate the right patterns, and relatively simple equations can lead to a great variety of patterns with small parameter changes). However, even though we obtain the patterns we observe in nature, this does not mean that we have captured the biological mechanism at work. There is a good example of the heated debates that can ensue regarding the plausibility of mathematical models in the book, "Modeling Differential Equations in Biology" Taubes (2001). Here, Taubes presents a series of three articles discussing a reaction-diffusion model for the formation of patterns in angelfish that disagree on the applicability of the model, and alternatives that would yield similar results.

Our knowledge about the science behind pattern formation has been slower to develop than the creation of mathematical models. In part, this is due to the fact that it is hard to isolate individual molecules and study their role in biological mechanisms. Many of the pattern formation models we have discussed assume that there exist chemicals in developing embryos that will react in certain ways, but it is much easier to posit the existence of such chemicals than to find them, isolate them, and test that they do what the models predict. In the end, it is not enough to have just the experiments or just the math. Mathematical models can help shape and direct the experimental design, and the results can then be used to update, change or discard the model.

One of the difficulties of modeling pattern formation is that it is generally not possible to analytically solve the reaction-diffusion systems that describe the dynamics of the interacting chemical species. As shown in this paper, it is necessary to study the system by linearizing about the steady state and checking for the Turing conditions, and if that is not sufficient asymptotic techniques must be applied. As a result, every new reaction-diffusion system that is proposed has to be analyzed and simulated before it is fully understood, and this can be a slow process. Ideally, these models could be used by experimentalists in order to make predictions about a biological system that presents patterns. Nonetheless, variations of the same reaction-diffusion equation nonetheless requires the full analysis to be carried out again, and the difficulty of doing so has hindered the efforts to update the models as new experimental evidence is collected.

One of the ongoing efforts is to find methods of analyzing reaction-diffusion equations that are easier to carry out, but that still captures the dynamics of the system. One such method is the Local Pulse Analysis proposed by Walther et al. (2012), , which looks at a single reaction-dfifusion systems and using bifurcation theory looks at the different behaviors of the system with different parameter values. Interestingly, they find that the analysis can yield a more global view of the model's repertoire of dynamics and using this, parameter ranges for which a system will have Turing patterns and where it will have parameters due to other types of instabilities. Methods like Local Pulse Analysis promise to facilitate the collaboration between applied mathematics and the natural sciences in the future.

7. Appendix: The website

Project site: http://www.theshapeofmath.com/princeton/dynsys

As mentioned in the Introduction, this paper accompanies a website that was created so that students with less mathematical background could still access the concepts and intuitions of pattern formation. The website was created in such a way that it could be read from beginning to end like any set of course notes, or a chapter in a textbook. Students with a general interest in pattern formation, and some mathematical background should be able to go to the website and gain a better understanding of the mathematical, physical, and historical ideas behind models of pattern formation.

In addition, since the website contains a wide variety of multimedia material, it can be used as teaching aids in a dynamical systems course in order to supplement the lectures. The integration of the website to a classroom environment can be accomplished in several ways, for example:

1. Students can read through the relevant pages, so that they arrive to class with a grasp on the intuitive ideas and can understand the mathematical analysis more readily.
2. Videos can be played at the beginning of the class
3. The animations can be used by instructors to supplement lecture slides, and students can refer to them and listen to the audio accompaniments when they are home to refresh their memory.
4. The MATLAB demos and the embedded code can help students understand how the animations are created and serve as a primer to the field of numerical methods.

The website contains:

- Eight YouTube videos (approximately 4-5 minutes each) covering different topics that were animated in Flash
- GIF animations accompanied by an audio explanation
- Notes covering material similar to that of this paper

References

(2014). *diffuse, v.* Oxford University Press, oed online edition.

Brown, R. (1828). Xxvii. a brief account of microscopical observations made in the months of june, july and august 1827, on the particles contained in the pollen of plants; and on the general existence of active molecules in organic and inorganic bodies. *The Philosophical Magazine, or Annals of Chemistry, Mathematics, Astronomy, Natural History and General Science*, 4(21):161–173.

Cooper, S. B. and Maini, P. K. (2012). The mathematics of nature at the Alan turing centenary. *Interface Focus*, 2(4):393–396.

Crick, F. (1970). Diffusion in embryogenesis. *Nature*, 225:420–422.

D'Arcy, W. T. (1992). *On growth and form: The complete revised edition*. Dover, New York.

Einstein, A. (1956). *Investigations on the Theory of the Brownian Movement*. Dover Publications.

Gierer, A. and Meinhardt, H. (1972). A theory of biological pattern formation. *Kybernetik*, 12(1):30–39.

Kharab, A. and Guenther, R. B. (2006). *An introduction to numerical methods: a MATLAB approach*. Boca Raton: Chapman & Hall, 2 edition.

Kondo, S. (2009). How animals get their skin patterns: fish pigment pattern as a live turing wave. *Int. J. Dev. Biol*, 53:851–856.

Little, S. C., Tkačik, G., Kneeland, T. B., Wieschaus, E. F., and Gregor, T. (2011). The formation of the bicoid morphogen gradient requires protein movement from anteriorly localized mrna. *PLoS biology*, 9(3):e1000596.

Lotka, A. J. (1925). *Elements of Physical Biology*. Williams & Wilkins Company, Baltimore.

Maini, P. K., Woolley, T. E., Baker, R. E., Gaffney, E. A., and Lee, S. S. (2012). Turing's model for biological pattern formation and the robustness problem. *Interface Focus*, 2(4):487–96.

Mehrer, H. and Stolwijk, N. A. (2009). Heroes and highlights in the history of diffusion. *Diffusion Fundamentals*, 11:1–32.

Munafo, R. P. (1998). Reaction-diffusion by the Gray-Scott model: Pearson's parametrization. http://mrob.com/pub/comp/xmorphia.

Murray, J. and Sperb, R. (1983). Minimum domains for spatial patterns in a class of reaction diffusion equations. *Journal of mathematical biology*, 18(2):169–184.

Murray, J. D. (1981). On pattern formation mechanisms for lepidopteran wing patterns and mammalian coat markings. *Philos Trans R Soc Lond B Biol Sci*, 295(1078):473–96.

Murray, J. D. (1988). How the leopard gets its spots. *Scientific American*, 258(3):80–87.

Murray, J. D. (2003). *Mathematical Biology II: Spatial Models and Biomedical Applications*, volume 2. Springer-Verlag, New York.

Murray, J. D. and Myerscough, M. R. (1991). Pigmentation pattern formation on snakes. *J Theor Biol*, 149(3):339–60.

Nakamasu, A., Takahashi, G., Kanbe, A., and Kondo, S. (2009). Interactions between zebrafish pigment cells responsible for the generation of turing patterns. *Proc Natl Acad Sci U S A*, 106(21):8429–34.

Nelson, E. (1967). *Dynamical theories of Brownian motion*, volume 10. Princeton University Press, Princeton.

Taubes, C. (2001). *Modeling differential equations in biology*. Prentice Hall, Upper Saddle River.

Turing, A. (1952). The chemical basis of morphogenesis. *Philosophical Transactions of the Royal Society of London Series B-Biological Sciences*, 237:37–72.

Walther, G. R., Marée, A. F., Edelstein-Keshet, L., and Grieneisen, V. A. (2012). Deterministic versus stochastic cell polarisation through wave-pinning. *Bulletin of mathematical biology*, 74(11):2570–2599.

I pledge my honor that this paper represents my own work in accordance with Princeton University regulations.

Princeton Neuroscience Institute, Princeton University, NJ
E-mail address: teramoto@princeton.edu